

Faraday Discussions

Accepted Manuscript



This manuscript will be presented and discussed at a forthcoming Faraday Discussion meeting. All delegates can contribute to the discussion which will be included in the final volume.

Register now to attend! Full details of all upcoming meetings: <http://rsc.li/fd-upcoming-meetings>



This is an *Accepted Manuscript*, which has been through the Royal Society of Chemistry peer review process and has been accepted for publication.

Accepted Manuscripts are published online shortly after acceptance, before technical editing, formatting and proof reading. Using this free service, authors can make their results available to the community, in citable form, before we publish the edited article. We will replace this *Accepted Manuscript* with the edited and formatted *Advance Article* as soon as it is available.

You can find more information about *Accepted Manuscripts* in the [Information for Authors](#).

Please note that technical editing may introduce minor changes to the text and/or graphics, which may alter content. The journal's standard [Terms & Conditions](#) and the [Ethical guidelines](#) still apply. In no event shall the Royal Society of Chemistry be held responsible for any errors or omissions in this *Accepted Manuscript* or any consequences arising from the use of any information it contains.

Parameter free calculation of the subgap density of states in poly(3-hexylthiophene)

Jarvist M. Frost^{1,2}, James Kirkpatrick^{1,3}, Thomas Kirchartz^{1,4}, and Jenny Nelson^{1*}

5 DOI: 10.1039/b000000x [DO NOT ALTER/DELETE THIS TEXT]

¹Department of Physics and Centre for Plastic Electronics, Imperial College London, London SW7 2AZ, United Kingdom

10 ²Department of Chemistry, University of Bath, Claverton Down, Bath BA2 ..., United Kingdom

³Department of Physics, Oxford University, Parks Road, Oxford OX1 3LB, United Kingdom

⁴IEK-5 Photovoltaics, Forschungszentrum Juelich, D- Juelich, Germany

15

Abstract

We investigate the influence of intra-chain and inter-chain interactions on the subgap density of states in a conjugated polymer using a combination of atomistic molecular dynamics simulation of polymer film structure and tight-binding calculation of electronic energy levels. For disordered assemblies of poly-3-hexylthiophene we find that the tail of the density of hole states is approximately exponential with a characteristic energy of 37 meV, which is similar to experimental values. This tail of states arises mainly from variations in the electronic coupling between neighbouring monomers, and is only slightly influenced by interchain coupling. Thus, knowledge of the disorder in torsion between neighbouring monomers is sufficient to estimate the density of states for the polymer. However the intrachain torsional disorder is determined largely by the packing of the chains rather than the torsional potential alone. We propose the combination of methods as a tool to design higher mobility conjugated polymers.

Introduction

Organic semiconductors are promising materials for electronic and optoelectronic applications such as transistors,¹ light emitting diodes² and solar cells.³⁻⁷ Among the key parameters of importance for these applications are the mobility of charge carriers and, in bipolar devices, the charge carrier lifetime. In most organic semiconductors charge transport is controlled by the molecular nature of the material such that charges are localised on individual molecules or conjugated segments and move between weakly coupled sites via a hopping process. The variability in molecular conformation and packing which naturally arises in these soft materials then gives rise to variability in the energy of the states on which charge carriers reside (so called 'energetic disorder'), and variability in the separation and relative orientation of conjugated units (so called 'configurational disorder') both of which tend to slow down transport by trapping charges^{8,9}. Localized states in the electrical gap [of organic semiconductors] are also expected to increase the rate of non-radiative electron - hole recombination in bipolar devices such as solar cells.¹⁰ Energetic disorder can be described in terms of a density of (localised) states (DoS). In principle, both the charge carrier mobility and lifetime, and their charge density dependence, are functions of the DoS.¹¹ In order to optimise and diagnose device performance and to develop materials of improved electrical properties it is essential to develop an improved understanding of the origin of localized states in organic semiconductors.

A variety of experimental studies of organic semiconductors indicate the presence of a tail of states that extends into the electrical gap. Most commonly the density N of localized states in disordered organic semiconductors is approximated by either a Gaussian distribution⁹ or an exponential tail¹²⁻¹⁴. In the case of an exponential tail of electron states, the density of states N in energy interval dE is given by

$$N(E) dE = N_0 \exp\left(\frac{E - E_c}{E_{ch}}\right) dE.$$

30

(1)

where E is the energy, E_c is a reference energy at which electrons are free to move, which we will refer to as the mobility edge, N_0 is the density of states at E_c and E_{ch} is the characteristic energy of the tail. This characteristic energy is the key parameter controlling the influence of localized states on device performance, such that higher values of E_{ch} lead to larger concentrations of deep lying states that can trap charges, slow down transport and facilitate recombination.^{15, 16}

These tails of states have been studied with a wide range of techniques, in unipolar devices such as transistor structures^{17, 18, 19}, and especially in bipolar devices such as OLEDs and solar cells. Evidence for a roughly exponential tail of localized states in disordered polymer:fullerene blends used for organic solar cells comes from measurements of the absorption edge using quantum efficiency or spectral

photoconductivity methods,^{10, 20, 21} transient photocurrent measurements^{11, 22-24}, transient absorption measurements,^{25, 26} charge extraction measurements²⁷⁻³⁰ and space charge limited current measurements.³¹ The largest body of experimental evidence exists for the blend poly (3-hexylthiophene) (P3HT): 1-(3-methoxycarbonyl)propyl-1-phenyl-[6,6]-methano fullerene (PCBM). For that system, transient absorption measurements indicate tails states with E_{ch} in the range of 35 meV to 70 meV,³²⁻³⁴ transient photocurrent measurements also indicate E_{ch} in the range of 35 meV to 65 meV.¹¹ and sub-gap quantum efficiency measurements suggest E_{ch} between 37 meV (at 300 K) and 32 meV (at 200 K).²⁰ Although the value of E_{ch} varies between measurements and with different processing regimes³²⁻³³ the data converge on a consensus of approximately exponential behaviour with E_{ch} in the range of 35 to 65 meV. Temperature dependent quantum efficiency and transient photocurrent measurements further suggest that the tail of states is temperature dependent.²⁰

15

Localised intra-gap (or trap) states in conjugated polymers may arise from chemical or physical defects. Possible chemical defects include in-chain defects such as end groups, sp^3 configured carbon atoms, or oxidised species as well as leaving groups or small molecular weight components remaining from synthesis. Physical defects may result from variations in the conformation of the conjugated backbone and in intermolecular interactions. Whilst chemical impurities can largely be eliminated by purification and fractionation of polymers and choice of end groups, disorder in conformation and packing cannot be avoided in an organic semiconductor film. Amongst the configurational parameters that can influence the energies of electron and hole states in conjugated polymers, the torsion angle θ between consecutive units along the conjugated backbone is one of the most significant. For any compound the value of θ in the geometrically relaxed structure results from competition between the dispersion of pi-electron states through consecutive units, which tends to planarise the chain, and steric effects which tend to deplanarise it. The potential energy profile for rotation of the units around this energetic minimum tends to be relatively soft, presenting a barrier of order 100 meV to chain rotation^{35,36} and thus allowing substantial thermal fluctuations in θ at room temperature. Note that such fluctuations might be expected to make the DoS temperature dependent. In a solid polymer film at room temperature, torsion angles are further disrupted by steric effects in molecular packing and by chain folding. The net disorder in θ results in disorder in the extent of conjugated segments and in the energy of the electronic states³⁶. As well as this intrachain coupling, as controlled by θ , some contribution to the spatial extent and energy of electronic states may arise from electronic coupling between conjugated units in neighbouring chains. Such interchain coupling may be expected especially in crystalline materials with a strong degree of pi stacking.

Whilst the concept that torsional disorder and packing disorder can give rise to disorder in electronic states energies is well known, attempts to derive the DoS for realistic molecular assemblies are limited to date. A number of studies report distributions of states for assemblies of small molecules such as fullerenes calculated using quantum chemical methods^{37, 38} but these methods are limited to relatively small assemblies. The problem is more challenging for polymers where the effect of torsion on strong intrachain coupling and of position on weak intrachain

coupling must be included. Most studies of P3HT to date have addressed ordered systems. Cheung and co-workers have studied the variation in torsion distribution that results from dynamic chain fluctuations in crystalline P3HT and relate this to charge transport³⁹. Rivnay considered the effect of variations in chain spacing, as deduced from x-ray diffraction studies, on tail states in P3HT, assuming a Gaussian distribution of separations⁴⁰. More recently Poelking and co-workers derived a density of states for disordered crystalline P3HT of different regioregularity resulting from fluctuations in the intermolecular spacings⁴¹. Whilst understanding of the DoS in the crystalline fraction of P3HT is certainly useful, charge transport in devices is likely to be rate-limited by trapping in gap states within the larger, non-crystalline fraction of the polymer film.

In this paper we will consider the relative importance of both inter- and intra-chain contributions to the density of states in highly disordered films of P3HT. We use atomistic molecular dynamics (MD) to model the morphology of an assembly of regioregular thiophene oligomers of length 16 (corresponding to a low molecular weight of ca 3 kDa). Including both inter- and intra-chain coupling we find that the tail of the DoS at room temperature is approximately exponential with a characteristic energy of approximately 37 meV, similar to the lower range of experimental values reported.^{20, 21} More importantly, we are also able to resolve the contributions of inter- and intra-molecular coupling to the density of states, finding that this deep tail results mainly from intra-chain coupling and thus results mainly from torsional disorder of the polymer backbone rather than positional, packing, disorder. We also find that this deep tail is temperature dependent. Finally we show that models that rely on a Gaussian distribution of interchain separations are likely to invoke unphysically close minimum separations. We argue that one route to materials with lower energetic disorder is to design stiffer polymers with less torsional freedom.

Methods

The empirical forcefield used for molecular dynamics was derived from the parameters developed by Moreno et al.,³⁵ supplemented with Optimized Potentials for Liquid Simulations (OPLS)⁴² as implemented in the GROMACS⁴³ molecular dynamics package. The starting geometry of 40 independent extended (3-hexylthiophene) hexadecamers were packed loosely into a 10 nm x 10 nm x 10 nm box with periodic boundary conditions using PACKMOL.⁴⁴ For the room temperature assemblies, steepest descent energy minimisation with the empirical forcefield was followed by an equilibration molecular dynamics run of 1 ns, with initial atomic velocities drawn from a 300 K Maxwell distribution and using the leapfrog integrator with a Berendsen thermostat and barostat at 300 K and 1 atm respectively. This resulted in the compression of the simulation volume from 1000 nm³ to 158 nm³ (density of 1.108 g/cm³). Molecular dynamics was continued for a further 50 ns, with simulation coordinates captured from snapshots taken every 10 ps. Densities of states were computed from over 3000 such snapshots. A typical snapshot is shown in Figure 1.

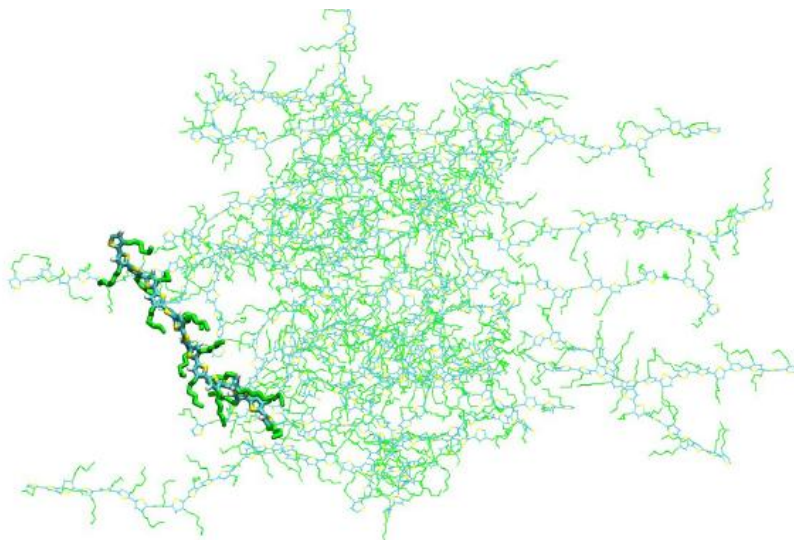


Figure 1: Typical assembly of 3HT hexadecamers generated using molecular dynamics at 300K.

The role of inter- and intra-molecular transfer integrals is assessed by looking at three different cases: (a) *Intermolecular only* where each oligomer is considered as a single charge transport unit with given energy. All intermolecular couplings are computed and the resulting tight-binding Hamiltonian is solved, to deduce the distribution of eigenvalues and hence, the density of states. (b) *Intramolecular only*, where each oligomer is decomposed into a set of monomers coupled only to its immediate neighbours via a θ dependent transfer integral. A tight-binding Hamiltonian is solved for each oligomer and the set of results collected to give the average density of states, and (c) *Inter and Intra-molecular* where each monomer in the whole simulation box contributes to the basis set for the tight binding Hamiltonian. All inter- and intra- molecular couplings are computed between all monomers resulting in a large Hamiltonian which is diagonalised, yielding the density of states.

Once an MD trajectory has been computed, we use the VOTCA charge transport toolkit (votca-ctp)^{45, 46} to map conjugated segments on to the oligomers simulated with molecular dynamics. The inter-chain transfer integrals are computed using molecular orbital overlap⁴⁷ from semi-empirical INDO/S Highest Occupied Molecular Orbitals. In the case of the inter-chain only computation (case (a)), orbitals for relaxed hexadecamers are mapped on to the oligomers generated by MD and used to compute the transfer integrals between different oligomers. In the case of the inter- and intra- chain coupling (case (c)), orbitals for relaxed monomers are mapped on to the coordinates of each monomer in the MD generated assembly and coupling between monomers located on different oligomers are computed using VOTCA.

Intra-chain inter-monomer electronic coupling terms, needed for both cases (b) and (c) cannot be computed from molecular orbital overlap. In these cases the coupling is assumed to depend only on the torsion angle ϕ between neighbouring monomers

according to the form

$$J_{\text{intra}} = J_0 \cos(\theta) \quad (2)$$

We compute J_0 by calculating the HOMO for planar thiophene oligomers of 5 different number N of repeat units using DFT with a B3LYP functional and a double split 6-31g* basis set. We then fit the N -dependent trend in HOMO energy to the form expected from a tight-binding calculation for a chain of identical units coupled by J_0 . This procedure yields a value of 0.8 eV for J_0 .

10 Once all the electronic couplings are computed, we set up the Huckel Hamiltonian

$$H = |i\rangle\langle i| \varepsilon_i + \sum_j \left(J_{i,j} |i\rangle\langle j| + t_{i,j}^* |j\rangle\langle i| \right) \quad (3)$$

where the diagonal element ε_i is set to a single value E_0 . Here we set $E_0 = -5.0$ eV, in accordance with the approximate ionization potential for P3HT of 5.0 eV ⁴⁸. We find 15 the eigenvalues of this Hamiltonian using standard GNU Scientific Library solvers and the repeat the process for at least 3000 snapshots of the equilibrated oligomer assembly. The eigenvalues from all snapshots are stored and compiled into distributions representing the DoS functions for the different cases studied.

20 To repeat the process to study the electron rather than the hole DoS, we would replace the J_0 extracted from the length dependence of the HOMO as calculated by DFT with the value extracted from the oligomer length dependence of the LUMO.

Results and Discussion

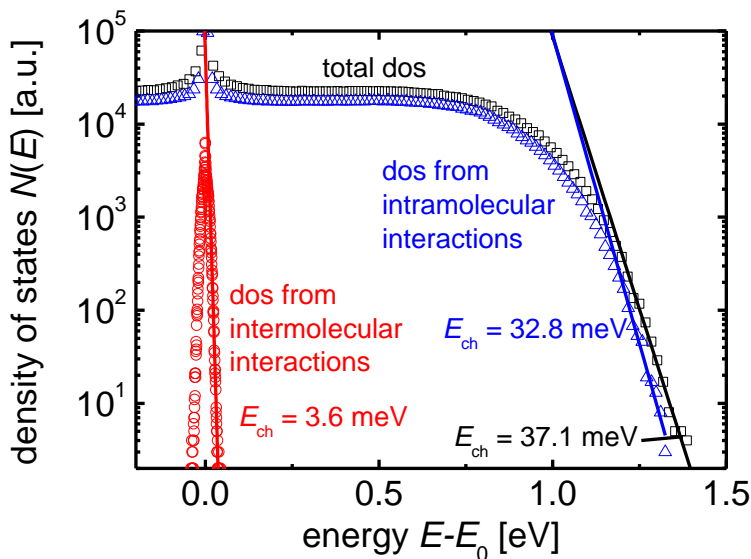


Figure 2. DoS for molecular assemblies equilibrated at a temperature of 300K calculated for the cases of intra-oligomer coupling only (circles), inter-monomer coupling only (triangles) and both intra- and inter-monomer coupling (squares). Straight lines represent exponential fits to the tail of states. Energy is measured up from the energy of the thiophene HOMO used in the calculation ($E_0 = -5.0$ eV).

In Figure 2 the resulting DoS for the three cases for assemblies generated at 300K are compared. The DoS for case (a) including inter-chain couplings only (open circles) is very sharp, and an exponential fit to the tail reveals a characteristic energy of only 3.6 meV. In contrast, when intra chain couplings only are considered (open triangles) or when both inter- and intra-chain couplings are included (open squares) a much broader tail in the DoS is obtained. The deep part of this tail can be fit to an exponential tail, with a characteristic energy of 35 meV for the case of only intra-chain couplings (case b) and around 37 meV for case (c), with both types of coupling. These values are in good agreement with values of E_{ch} obtained from subgap quantum efficiency measurements on P3HT:PCBM solar cells^{20, 21} and with the lower values obtained from transient photocurrent and transient absorption studies. However, our results show that, in contrast to some previous studies^{20, 40}, interchain interactions alone cannot explain the breadth of the density of localised hole states in P3HT. The interchain interactions do affect the tail of the DoS slightly, possibly because tail states will tend to result from planarised segments and interchain couplings will tend to be strongest between neighbouring, cofacial planar segments.

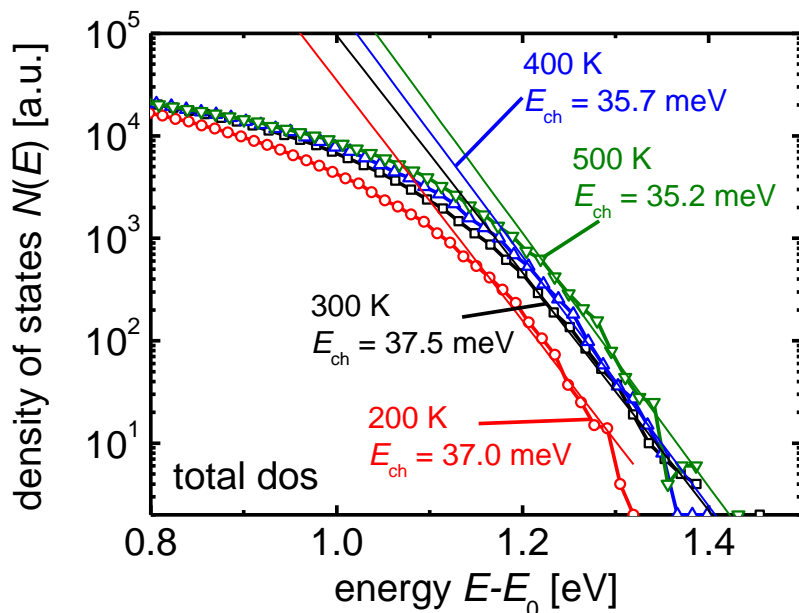
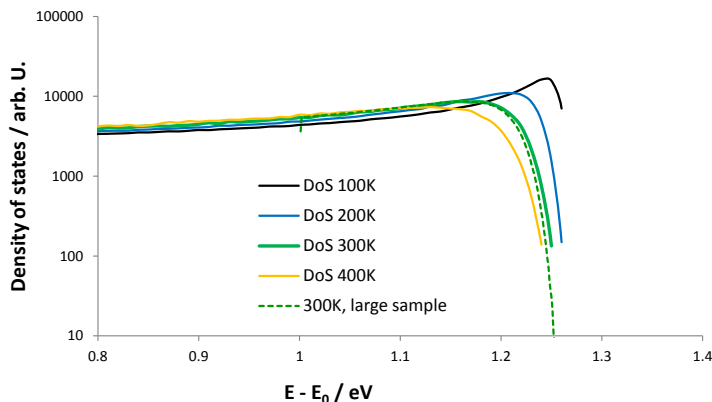


Figure 3: Calculated DoS due to both intra- and inter-monomer coupling, as a function of temperature. Straight lines represent exponential fits to the tail of states. The slope of the deep part of the tail is insensitive to temperature. Energy is measured up from the energy of the thiophene HOMO used in the calculation ($E_0 = -5.0$ eV).

Figure 3 shows the DoS obtained from both intra and intermolecular coupling for assemblies generated at different temperatures. We would expect the range of torsion angles present in the ensemble to broaden with increasing temperature as increasing kT increases the probability of configurations further from the energetic minimum. The range of torsional angles does indeed broaden (see Figure S1(a) in the supporting information) and, accordingly, the DoS becomes broader with increasing temperature. However the value of E_{ch} obtained from an exponential fit to the deep tail of the DoS is relatively invariant with temperature. It should be noted that the tail is not perfectly exponential and a fit to the DoS higher in the tail would yield values that slowly increase with temperature. The effect of temperature on the interchain-only DoS is also very weak (Figure S2 in Supporting Information). The close agreement between the DoS obtained in cases (b) and (c), when the coupling between monomers on different chains are excluded and included, suggests that the DoS for the disordered polymer film may be explained solely by the distribution of inter-monomer torsion angles. This distribution will be influenced both by the size of thermally enabled torsional fluctuations and by chain distortion resulting from the dense packing of the chains and their mutual repulsion. To investigate the extent to which the thermal fluctuations alone control the DoS we implemented a simple, linear tight binding scheme whereby the torsion angle between neighbouring monomers was drawn from a thermally generated distribution of angles $f(\theta)$. We obtain $f(\theta)$ by mapping a Boltzmann distribution of torsional

potential energies $g(U(\theta)) = A \exp(-U(\theta)/kT)$ on to θ , where we have approximated $U(\theta)$ by $U_0 \sin^2(\theta)$, with $U_0 = 0.126$ eV, fitted to published torsional potential³⁵. The angular distributions generated this way are broader than those extracted from the MD and are more strongly temperature dependent (Fig S1(a) and (b) in Supporting Information). We then populate the off-diagonal elements of the Hamiltonian with coupling terms corresponding to the selected values of θ using eq. (2), and solve for the eigenvalues.



10 **Figure 4.** DoS resulting from the linear chain thermodynamic model for chains of 10^6 monomers at different temperatures. Although the DoS is broad, tails are much sharper than from the torsional distributions generated by MD, meaning that long conjugated segments are more likely. The 300K DoS is calculated for a large chain of 10^8 monomers for comparison, showing that the DoS tail shape is insensitive to sample size over this range,

15 The resulting temperature dependent eigenvalue distributions (Figure 4) show that the tails of states generated by this method are relatively sharp compared to those obtained from the MD generated torsional configurations, and are too narrow to explain the experimental DoS. This tells us that, whilst the DoS in the disordered film may be dominated by intramolecular torsional variations rather than
 20 intermolecular coupling, these torsional variations are controlled by factors other than the torsional potential between conjugated rings. In the MD generated assembly, the distribution of θ is influenced also by the interactions between side chains, repulsive forces at close atomic separations that may constrain the molecule into thermodynamically unfavourable conformation (see Fig. S3 in the SI), and by
 25 face-on interactions with neighbouring conjugated segments, that will tend to planarise the chain. The atomistic MD exercise is necessary to capture these phenomena and so explain the breadth of the observed DoS. A comparison of the DoS tails for the simple thermodynamic model and the MD model suggests that the occurrence of long conjugated segments that act as traps is more rare in the realistic,
 30 MD case.

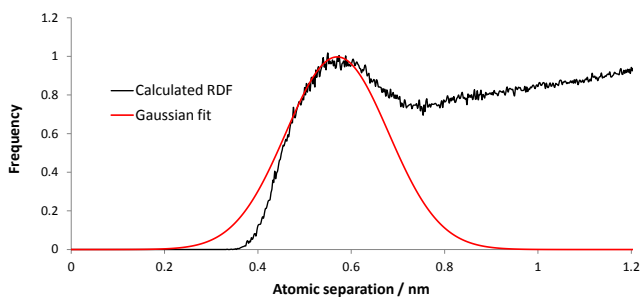


Figure 5. Radial distribution function for the closest approach of monomers located on different oligomers (black line) and a Gaussian fit to the first peak of the function. The Gaussian function is a poor fit at very small separations.

Finally we use our findings to address the validity of the Gaussian disorder model for inter-molecular distances. Following early approaches to including disorder in electronic coupling into models of charge transport in organic semiconductors⁹ several groups have invoked a Gaussian distribution in interplane distances to explain electronic phenomena^{20, 40}. **Figure 5** shows the probability distribution function of finding an intermolecular neighbour at a certain distance as calculated by molecular dynamics. Also shown is a fit to the tail of this probability density function with a Gaussian distribution. The Gaussian model appears to be a good approximation, except for at short distances (less than 0.4 nm) where the van der Waals repulsion becomes strong and the atoms must not overlap. In the atomistic MD simulation, small inter-chain distances are much less likely than in a Gaussian disorder model, meaning that large inter-chain integrals are also less likely and, therefore, fewer sub-band gap states are expected to result from intermolecular interactions. This observation can resolve the apparent contradiction between our findings and those of previous studies^{20, 40}.

Conclusions

Using a combination of atomistic molecular dynamics and a tight-binding calculation of hole state energies, we have found that the tail of the density of hole states in P3HT follows an exponential form with a characteristic energy of around 35-40 meV. This value agrees well with values observed experimentally using sub-gap quantum efficiency measurements and it lies at the lower end of the range of values observed using transient absorption and photocurrent measurements. The breadth of the tail of states arises mainly from intra-molecular electronic couplings, which are generally much stronger than interchain couplings. The tail states in this picture thus result from extended planar segments. The key conclusion is that intrachain torsional disorder can account for a significant fraction of the disorder observed experimentally whilst disorder in interchain coupling, at least in the non-crystalline parts of the polymer film, cannot. Deeper tail state distributions often observed in practice for P3HT may be influenced by chemical defects, polydispersity, nanocrystallinity or other factors not included in our model.

The finding that the distribution of tail states is dominated by intra-chain coupling elements and the simple $\cos(\theta)$ torsional dependence of such elements means that, in general, the density of tail states for a conjugated polymer could be estimated from a representative distribution of torsion angles via a simple tridiagonal tight binding Hamiltonian. The generation of such a representative ensemble of torsional angles still requires some realistic – and therefore time consuming – simulation of the polymer chain assembly. We have shown here for the case of 3HT oligomers that the disorder in intrachain torsion responsible for the distribution of tail states results from the way in which the chains are packed in the solid film and cannot be predicted solely from knowledge of the torsional potential barrier in the conjugated backbone. This reflects the fact that the molecular microstructure within polymer films is normally far from equilibrium.

Regarding practical routes to narrow the distribution of tail states in conjugated polymers, this work suggests that a central focus should be on designing stiffer polymers with higher potential barriers to oppose torsional disorder. However to make the most of such planarising structures, process routes should allow the chains to find configurations where chain conformation more closely reflects the built-in potential. Improving the organization and crystallinity of a polymer is also likely to affect the density of states, but mainly as a consequence of the increase in intrachain order.

Acknowledgements

T. K. acknowledges support by an Imperial College Junior Research Fellowship. JN acknowledges the Royal Society for a Wolfson Merit Award, and the Engineering and Physical Sciences Research Council for support via grants [EP/K029843/1](#), [EP/G031088/1](#), [EP/J017361/1](#).

† Electronic Supplementary Information (ESI) available: [details of any supplementary information available should be included here]. See DOI: 10.1039/b000000x/

(a) References

1. R. Noriega, J. Rivnay, K. Vandewal, F. P. V. Koch, N. Stingelin, P. Smith, M. F. Toney and A. Salleo, *Nat Mater*, 2013, **12**, 1038-1044.
2. S. Reineke, F. Lindner, G. Schwartz, N. Seidler, K. Walzer, B. Lussem and K. Leo, *Nature*, 2009, **459**, 234-U116.
3. G. Li, R. Zhu and Y. Yang, *Nat Photonics*, 2012, **6**, 153-161.
4. L. T. Dou, J. B. You, J. Yang, C. C. Chen, Y. J. He, S. Murase, T. Moriarty, K. Emery, G. Li and Y. Yang, *Nat Photonics*, 2012, **6**, 180-185.
5. Z. C. He, C. M. Zhong, S. J. Su, M. Xu, H. B. Wu and Y. Cao, *Nat Photonics*, 2012, **6**, 591-595.
6. M. Graetzel, R. A. J. Janssen, D. B. Mitzi and E. H. Sargent, *Nature*, 2012, **488**, 304-312.
7. J. Nelson, *Materials Today*, 2011, **14**, 462-470.
8. A. Salleo, *Materials Today*, 2007, **10**, 38-45.
9. H. Bässler, *physica status solidi (b)*, 1993, **175**, 15-56.
10. R. A. Street, A. Krakaris and S. R. Cowan, *Adv Funct Mater*, 2012, **22**, 4608-4619.
11. R. A. Street, *Phys Rev B*, 2011, **84**, 075208.
12. M. H. Cohen, H. Fritzsche and S. R. Ovshinsky, *Phys Rev Lett*, 1969, **22**, 1065-1068.
13. G. D. Cody, T. Tiedje, B. Abeles, B. Brooks and Y. Goldstein, *Phys Rev Lett*, 1981, **47**, 1480-1483.
14. T. Tiedje, J. M. Cebulka, D. L. Morel and B. Abeles, *Phys Rev Lett*, 1981, **46**, 1425-1428.
15. C. Vanberkel, M. J. Powell, A. R. Franklin and I. D. French, *J Appl Phys*, 1993, **73**, 5264-5268.
16. T. Kirchartz and J. Nelson, *Phys Rev B*, 2012, **86**, 165201.

17. A. R. Völkel, R. A. Street and D. Knipp, *Physical Review B*, 2002, **66**, 195336.
18. C. Tanase, E. J. Meijer, P. W. M. Blom and D. M. de Leeuw, *Physical Review Letters*, 2003, **91**, 216601.
19. I. N. Hulea, H. B. Brom, A. J. Houtepen, D. Vanmaekelbergh, J. J. Kelly and E. A. Meulenkamp, *Physical Review Letters*, 2004, **93**, 166601.
20. R. A. Street, K. W. Song, J. E. Northrup and S. Cowan, *Phys Rev B*, 2011, **83**, 165207.
21. W. Gong, M. A. Faist, N. J. Ekins-Daukes, Z. Xu, D. D. C. Bradley, J. Nelson and T. Kirchartz, *Phys Rev B*, 2012, **86**, 024201.
22. N. Christ, S. W. Kettlitz, S. Zuefle, S. Valouch and U. Lemmer, *Phys Rev B*, 2011, **83**, 195211.
23. R. C. I. MacKenzie, C. G. Shuttle, M. L. Chabinye and J. Nelson, *Advanced Energy Materials*, 2012, **2**, 662-669.
24. C. G. Shuttle, N. D. Treat, J. D. Douglas, J. M. J. Frechet and M. L. Chabinye, *Advanced Energy Materials*, 2012, **2**, 111-119.
25. J. Nelson, in *Phys Rev B*, 2003, p. 155209.
26. M. Tachiya and K. Seki, *Phys Rev B*, 2010, **82**, 085201.
27. C. G. Shuttle, A. Maurano, R. Hamilton, B. O'Regan, J. C. de Mello and J. R. Durrant, *Appl Phys Lett*, 2008, **93**, 183501.
28. T. Kirchartz, B. E. Pieters, J. Kirkpatrick, U. Rau and J. Nelson, *Phys Rev B*, 2011, **83**, 115209.
29. R. C. I. MacKenzie, T. Kirchartz, G. F. A. Dibb and J. Nelson, *J Phys Chem C*, 2011, **115**, 9806-9813.
30. A. Foertig, J. Rauh, V. Dyakonov and C. Deibel, *Phys Rev B*, 2012, **86**, 115302.
31. Z. M. Beiley, E. T. Hoke, R. Noriega, J. Dacuna, G. F. Burkhard, J. A. Bartelt, A. Salleo, M. F. Toney and M. D. McGehee, *Advanced Energy Materials*, 2011, **1**, 954-962.

32. P. E. Keivanidis, T. M. Clarke, S. Lilliu, T. Agostinelli, J. E. Macdonald, J. R. Durrant, D. D. C. Bradley and J. Nelson, *The Journal of Physical Chemistry Letters*, 2010, **1**, 734-738.
33. Y. Kim, S. Cook, S. M. Tuladhar, S. A. Choulis, J. Nelson, J. R. Durrant, D. D. C. Bradley, M. Giles, I. McCulloch, C.-S. Ha and M. Ree, *Nat Mater*, 2006, **5**, 197-203.
34. C. G. Shuttle, B. Oâ€™Regan, A. M. Ballantyne, J. Nelson, D. D. C. Bradley and J. R. Durrant, *Physical Review B*, 2008, **78**, 113201.
35. M. Moreno, M. Casalegno, G. Raos, S. V. Meille and R. Po, *J Phys Chem B*, 2010, **114**, 1591-1602.
36. J. L. Bredas, G. B. Street, Themans and Andre, *Journal of Chemical Physics*, 1985, **83**, 1323-1329.
37. D. L. Cheung and A. Troisi, *The Journal of Physical Chemistry C*, 2010, **114**, 20479-20488.
38. B. M. Savoie, A. Rao, A. A. Bakulin, S. Gelinas, B. Movaghar, R. H. Friend, T. J. Marks and M. A. Ratner, *Journal of the American Chemical Society*, 2014, **136**, 2876-2884.
39. D. L. Cheung, D. P. McMahon and A. Troisi, *The Journal of Physical Chemistry B*, 2009, **113**, 9393-9401.
40. J. Rivnay, R. Noriega, J. E. Northrup, R. J. Kline, M. F. Toney and A. Salleo, *Phys Rev B*, 2011, **83**, 121306.
41. C. Poelking and D. Andrienko, *Macromolecules*, 2013, **46**, 8941-8956.
42. W. L. Jorgensen, J. D. Madura and C. J. Swenson, *J Am Chem Soc*, 1984, **106**, 6638-6646.
43. D. Van der Spoel, E. Lindahl, B. Hess, G. Groenhof, A. E. Mark and H. J. C. Berendsen, *Journal of Computational Chemistry*, 2005, **26**, 1701-1718.
44. L. Martinez, R. Andrade, E. G. Birgin and J. M. Martinez, *Journal of Computational Chemistry*, 2009, **30**, 2157-2164.
45. V. Ruehle, C. Junghans, A. Lukyanov, K. Kremer and D. Andrienko, *Journal of Chemical Theory and Computation*, 2009, **5**, 3211-3223.

-
46. V. Ruehle, A. Lukyanov, F. May, M. Schrader, T. Vehoff, J. Kirkpatrick, B. r. Baumeier and D. Andrienko, *Journal of Chemical Theory and Computation*, 2011, **7**, 3335-3345.
47. J. Kirkpatrick, *International Journal of Quantum Chemistry*, 2008, **108**, 51-56.
- 5 48. S. A. Catalogue.